Thermal conductivity from approach-to-equilibrium molecular dynamics

E. Lampin, Pier Luca Palla, P.A. Francioso, F. Cleri

Thermal conductivity from approach-to-equilibrium molecular dynamics

Cite as: J. Appl. Phys. **114**, 033525 (2013); https://doi.org/10.1063/1.4815945
Submitted: 04 April 2013 • Accepted: 01 July 2013 • Published Online: 19 July 2013

E. Lampin, P. L. Palla, P.-A. Francioso, et al.

JOURNAL OF APPLIED PHYSICS **114**, 033525 (2013)

Thermal conductivity from approach-to-equilibrium molecular dynamics

E. Lampin,[a] P. L. Palla, P.-A. Francioso, and F. Cleri
Institut d'Electronique, Microelectronique et Nanotechnologie (IEMN, UMR CNRS 8520), Université de Lille I, 59652 Villeneuve d'Ascq Cedex, France

(Received 4 April 2013; accepted 1 July 2013; published online 19 July 2013)

We use molecular dynamics simulations to study the thermal transport properties of a range of poor to good thermal conductors by a method in which two portions are delimited and heated at two different temperatures before the approach-to-equilibrium in the whole structure is monitored. The numerical results are compared to the corresponding solution of the heat equation. Based on this comparison, the observed exponential decay of the temperature difference is interpreted and used to extract the thermal conductivity of homogeneous materials. The method is first applied to bulk silicon and an excellent agreement with previous calculations is obtained. Finally, we predict the thermal conductivity of germanium and α-quartz. © *2013 AIP Publishing LLC*. [http://dx.doi.org/10.1063/1.4815945]

I. INTRODUCTION

Nanoscale effects on heat transport are expected to have a major role on heat dissipation in advanced semiconductor architectures and to improve the efficiency of novel thermoelectric materials. Measurements of heat transport are generally performed on a macroscopic scale, and give the global response of a multi-material structure, including the various interfaces and materials. Atomistic computer simulation of heat transport in nanoscale materials and interfaces can help to analyze the experiments, understand the size- and time-scale limiting effects, and assess relevant macroscopic models.[1] Modeling of heat transport at the atomic scale by molecular dynamics (MD) simulations has followed up to now two major approaches. The first one, called equilibrium MD,[2] is based on the quantification of the fluctuations of the heat current in a system equilibrated at a given temperature. A Green-Kubo or Einstein fluctuation relation is eventually used to extract the thermal conductivity of the bulk material. The second method, called non-equilibrium MD or direct method,[3] is based on establishing a steady-state heat current between a heat source and a heat sink, and thermal bulk conductivity or interface conductance are extracted, respectively, from the slope or the discontinuity in the temperature gradient.

In the present work, we develop a different approach, called AEMD for "approach-to-equilibrium" MD. The system is initially set out-of-equilibrium by delimiting a portion heated at a different temperature from the rest. The approach-to-equilibrium, i.e., the time evolution of the temperature difference between the two parts, is then monitored. It can be shown that, for most practical cases of interest, the temperature decay is exponential. The equilibrium is typically reached in a few tenths to hundreds of ps, and consequently, the computational cost is much reduced, compared to both the computation of an autocorrelation function, as in the equilibrium MD, and the establishing of a steady state thermal current, as in the non-equilibrium MD. Moreover, the AEMD method is based on the calculation of the average temperature over substantially extended portions of the atomistic system, instead of requiring a local definition of temperature over extremely small regions (<1 nm). Of course, one could calculate such "local" values in the course of the simulation, e.g., for the sake of comparison with other MD or continuum methods. However, it is worth noting that the local temperature definition is not necessary ingredient for the implementation of the method. As a further advantage, the absolute energy flux does not have to be known, thereby reducing the numerical noise of the simulation.

It is worth noting that the AEMD presented here is not completely a new method. Inspired by the experimental set up of the laser-flash method to measure macroscopic thermal diffusivity,[4] techniques based on the approach-to-equilibrium were already implemented by some authors as a practical alternative to the more conventional methods, most often in cases where computational convergence seemed difficult to reach.[5] However, the exponential temperature decay was just observed as a result without providing a theoretical basis, moreover without investigating the advantages and limitations of the method. In the present paper, we propose explicit formulas to extract the bulk conductivity from the decay time of the temperature difference. The equations are derived from the analytical solution of macroscopic Fourier's heat equation. The limits of this assumption have been addressed and taken into account in the application of the formulas to the MD results. The AEMD method is applied to a range of bulk materials having thermal conductivities ranging from good (silicon) to poor (α-quartz).

The present work is structured as follows: in Sec. II, we describe the molecular dynamics calculation of the approach-to-equilibrium. In Sec. III, we derive a relation between the decay time of the exponential temperature difference and the bulk conductivity, by comparison with the solution of the heat equation in the same conditions. In Sec. IV, we first validate the method on the determination of the conductivity of silicon. An excellent agreement with previous calculations is found. Afterwards we apply the method to predict the conductivity of poorer thermal conductors, namely germanium and α-quartz, for which corresponding numerical evaluations are not available.

[a]Electronic mail: evelyne.lampin@univ-lille1.fr

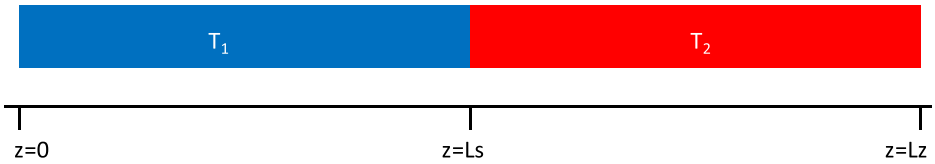

FIG. 1. An elongated box of length L_z and cross section S is periodised in the 3 directions. The atoms in the range $z \in [0;L_s]$ are heated to T_1, the atoms in the range $[L_s;L_z]$ are heated to T_2.

II. APPROACH-TO-EQUILIBRIUM MOLECULAR DYNAMICS

The principle of AEMD is to set an atomistic system out-of-equilibrium by imposing a temperature difference between two parts in contact; subsequently, the system is let evolve to its equilibrium, i.e., the temperature difference between the different parts of the system going to zero. In a typical case, a box is constructed to induce a preferential energy flow in the z-direction (see Fig. 1). Periodic boundary conditions are used in the three directions. Atoms in the interval $[z=0,L_s]$ are heated up to equilibrate at a temperature T_1, while atoms in the interval $[L_s,L_z]$ are heated to the temperature T_2. Afterwards the temperature controls are released, in order to create a directed energy flow that will bring the system to its equilibrium by a microcanonical, constant-{NVE} MD simulation. The initial equilibration of the two halves of the box ($L_s = L_z/2$) respectively at $T_1 = 600\,\mathrm{K}$ and $T_2 = 400\,\mathrm{K}$, is performed during 10 000 steps of 1 fs using the Nosé-Hoover thermostat.[6] This setting of the parameters leads to a target equilibrium temperature $T_{eq} = 500\,\mathrm{K}$. Si–Si and Ge–Ge interatomic forces are described using Tersoff potential,[7] the Si-O interactions in α-quartz are described using the BKS potential[8] within a modified version of the DL_POLY[9] code.

In classical MD simulations, all the vibrational degrees of freedom are excited at any temperature, i.e., energy is distributed according to the Maxwell-Boltzmann rather than the Bose-Einstein distribution. Therefore, MD simulations are meaningful only around or above the Debye temperature. This consideration motivates our choice of the target equilibrium temperature of 500 K (the Debye temperature being equal to 625 K for cSi (Ref. 10)).

Figure 2 gives an example of the temperature profiles at three subsequent snapshots of the MD simulation for the case of a crystalline silicon (cSi) box of dimensions $16a_0 \times 16a_0 \times 1100a_0 = 87 \times 87 \times 5993$ Å^3 ($a_0 = 5.45$ Å is the lattice parameter at the final temperature) containing 2 252 800 atoms. The square temperature profile corresponding to the initial equilibration of each block at distinct temperatures is labeled "0 ps" (red curve in Fig. 2). After 100 ps (green curve) the temperature profile becomes sinusoidal, and its amplitude decreases with time.

The temperature difference $\Delta T = T_1 - T_2$ between the two blocks is calculated every 50 steps and plotted in Figure 3. The time evolution of the $\Delta T(t)$ curve during the approach-to-equilibrium, $\Delta T \to 0\,\mathrm{K}$, can be fitted by a bi-exponential curve

$$\Delta T = c_1 \exp(-t/\tau_{Long}) + c_2 \exp(-t/\tau_{Trans}), \qquad (1)$$

where $c_1 = 183\,\mathrm{K}$, $c_2 = 14\,\mathrm{K}$, $\tau_{Long} = 225\mathrm{ps}$, $\tau_{Trans} = 23\mathrm{ps}$; the fit is also given in Fig. 3, light blue curve. As a general finding, the approach-to-equilibrium is always dominated by one single exponential over long times, together with a transient, short-lived contribution. In Sec. III, we provide an explanation for such multi–exponential behavior, and establish a way to extract the bulk conductivity from the $\Delta T(t)$ curve.

III. TEMPERATURE EQUILIBRATION IN A BULK MATERIAL

In the case of unidirectional (or 1-dimensional) heat transport, the heat equation governing the time and space evolution of the temperature, $T(t,z)$, derived from the Fourier law and from energy conservation, is

$$\frac{\partial T(t,z)}{\partial t} = \alpha \frac{\partial^2 T(t,z)}{\partial z^2}, \qquad (2)$$

where $\alpha = \kappa/C_V\rho$ is the thermal diffusivity (m^2 s^{-1}), κ is the thermal conductivity (W K^{-1} m^{-1}), C_V is the heat capacity (J K^{-1}), and ρ is the number density (m^{-3}). It is assumed that these quantities do not vary with time and space since we consider an homogeneous material, while their dependence on temperature is presumed to be slow over the temperature range considered, so as to be replaced by an average value. A solution of this equation can be obtained using separation of variables

$$T(t,z) = \theta(t).\zeta(z). \qquad (3)$$

In the particular case of a bulk system with periodic boundary conditions the temperature and flux are identical at $z = 0$

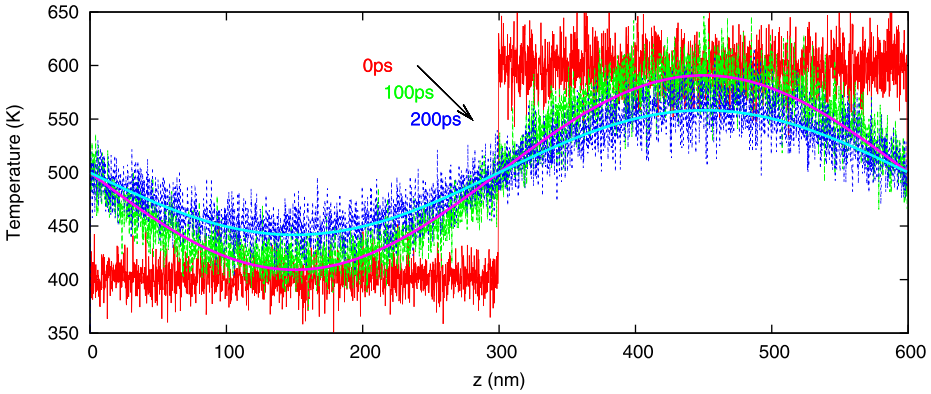

FIG. 2. Temperature profiles during AEMD at the beginning of {NVE} (red), after 100 ps (green) and 200ps (blue), and sine fit.

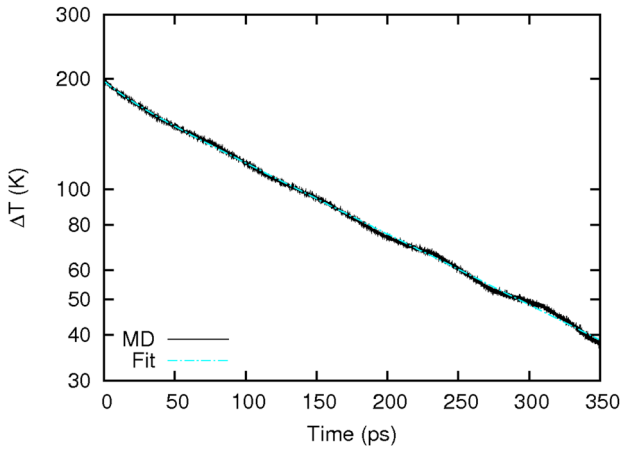

FIG. 3. Temperature difference between the two blocks versus time for the same system studied in Fig. 2 and its fits by Eq. (1).

and $z = L_z$. The time-dependent part of the solution is therefore $\theta(t) = \theta_0 \cdot \exp(-t/\tau_n)$ with

$$\tau_n = \frac{1}{4\pi^2 n^2}\frac{L_z^2}{\alpha} = \frac{1}{4\pi^2 n^2}\frac{L_z}{S}\frac{C_V}{\kappa}, \tag{4}$$

S being the transverse section with respect to the heat flow direction.

The complete solution is then given by

$$T(t,z) = \frac{A_0}{2} + \sum_{n=1}^{\infty}\left(A_n \cos(q_n z) + B_n \sin(q_n z)\right) e^{-t/\tau_n}, \tag{5}$$

where $q_n = 2\pi n/L_z$, n being an integer and

$$\begin{cases} A_n = \dfrac{2}{L_Z}\displaystyle\int_0^{L_Z} T(0,z)\cos(q_n z)dz \\ B_n = \dfrac{2}{L_Z}\displaystyle\int_0^{L_Z} T(0,z)\sin(q_n z)dz \end{cases} \tag{6}$$

correspond to the coefficients of the Fourier series of the initial condition. In the particular case where $L_s = L_z/2$, $T(0,z) = T_1$ for $0 < z < L_s$ and $T(0,z) = T_2$ for $L_s < z < L_z$, all the A_n and the B_n with n even are null, and the solution reads

$$T(t,z) = \frac{T_1 + T_2}{2} + \sum_{m=1}^{\infty}\frac{2(T_1 - T_2)}{(2m+1)\pi}\sin\left(\frac{2\pi(2m+1)}{L_z}z\right) \times e^{-(2m+1)^2 t/\tau_1}. \tag{7}$$

The corresponding expression of the average temperature difference between blocks $\Delta T(t)$ (plotted in Fig. 3) is

$$\Delta T(t) = \frac{1}{L_z/2}\int_0^{L_z/2} T(t,z)dz - \frac{1}{L_z/2}\int_{L_z/2}^{L_z} T(t,z)dz = \sum_{m=0}^{\infty}\frac{8(T_1 - T_2)}{(2m+1)^2\pi^2} e^{-(2m+1)^2 t/\tau_1}. \tag{8}$$

The general solution is therefore a multi-exponential function of time, with a dominant contribution of the first exponential decay time τ_1 ($m = 0$). The second exponential in the series has a decay time $\tau_2 = \tau_1/9$ and an amplitude 9 times smaller. Therefore, the terms for $m > 1$ are expected to have but a minor contribution in the approach to equilibrium, except during the transient since the terms for $m > 1$ enable the transition from the initial square profile to a sinusoidal one. Indeed, the temperature profile along z calculated by MD was already shown to have a sinusoidal form after 100 ps (Fig. 2).

During the transient, non-linear effects may also originate from strong gradients at the temperature step and make the solution deviate from Eq. (8). Nevertheless, we always extracted the thermal conductivity using the temperature decay at long times where temperature gradients are largely reduced. In these conditions, non-linear effects can be considered as negligible. This hypothesis has been verified by testing the dependence of the decay time on the fit range. A good stability of the results has been found starting the fit when $\Delta T(t) < \Delta T(0)/2$. The above considerations on transient can also explain the small discrepancy between the τ_1/τ_2 ratio predicted by the heat equation ($\tau_1/\tau_2 = 9$) and the corresponding ratio calculated by MD ($\tau_{Long}/\tau_{Trans} = 9.8$, Eq. (1)).

Identifying τ_{Long} with τ_1 (hereafter simply labeled τ), the bulk thermal conductivity can therefore be obtained from the relation in Eq. (4)

$$\kappa = \frac{1}{4\pi^2}\frac{L_z C_V}{S}\frac{1}{\tau}. \tag{9}$$

IV. BULK THERMAL CONDUCTIVITY OF cSI, cGE, AND α-quartz

We performed AEMD simulations with the method described in Sec. II for various bulk crystalline systems ranging from good to poor thermal conductors: cSi, cGe, and α-quartz, and for system lengths up to 1.2 μm. Various cross sections ranging from 4 × 4 to 16 × 16 (units of lattice parameter at the target temperature) were tested. Although the decay time already converges to a constant value for the smaller cross section (4 × 4), we used a higher section of 16 × 16 that presents a reduced numerical noise on the $\Delta T(t)$ curve, thereby permitting a higher precision in the determination of the decay time.

On the other hand, the heat capacity C_V was computed for each material following the approach of McGaughey and Kaviany.[11] The total energy E of a $8 \times 8 \times 8$ cubic cell is computed at $T = 490$, 495, 500, 505, and 510 K in the {NVT} ensemble, and averaged over 60 ps and 10 different initial conditions. The linear fit of $E(T)$ gives a specific heat per degree of freedom, $C_V/3Nk_B$, equal to 1.014 ± 0.013 for cSi, 1.024 ± 0.021 for cGe, and 1.196 ± 0.011 for α-quartz at $T = 500$ K.

First, the values of τ and C_V are obtained and combined according to Eq. (9) in order to calculate κ for silicon. The results of these calculations are summarized in Fig. 4. The uncertainty was systematically determined for each size following Zhou *et al.*[12]

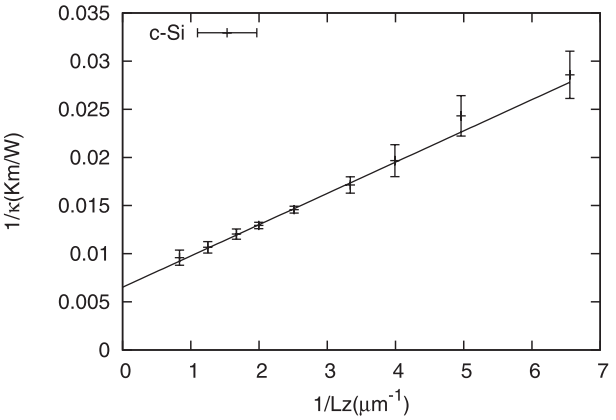

FIG. 4. System size dependence of $1/\kappa$ on $1/L_Z$ for cSi. The straight line is a fit with Eq. (10).

Results in Fig. 4 show a strong dependency of the conductivity on the system length. Such a behavior is expected due to the small size of the simulation box compared to some of the phonon mean free paths (MFP) of the infinite system. The convergence length issue was already raised by Sellan *et al.*,[13] who determined phonon MFPs greater than 10 μm in silicon at 500 K, such phonons contributing about 30% of the overall conductivity. Therefore, we have extrapolated the asymptotic conductivity by means of the Matthiessen's rule[3]

$$\frac{1}{\kappa} = \frac{1}{\kappa_\infty}\left(1 + \frac{\lambda}{L_z}\right), \tag{10}$$

with κ_∞ the asymptotic value of the thermal conductivity, and λ a length related to the phonon MFP.

The computational effort required by the present AEMD technique is drastically reduced compared to other numerical methods. Once the initial square temperature profile is equilibrated, the {NVE} MD simulation is performed during 100 ps to 1 ns, depending on the system size, up to attaining an accuracy for the asymptotic decay time of the order of a few percents. Therefore, bigger systems could be studied, of lengths up to 1.2 μm (about 4.5×10^6 of atoms with the 16×16 cross section). Such sizes are about 2 times longer and 10 times wider compared to previous calculations by Abs da Cruz *et al.*,[14] and 2 to 4 times longer and 4 times wider compared to Howell.[15] Nevertheless, due to computer limitations, the numerical improvement was not sufficient to attain the macroscopic limit for silicon. The extrapolation based on Eq. (10) gives $\kappa_\infty = 154 \pm 6$ W K^{-1}m^{-1} and $\lambda = 502 \pm 34$ nm.

Abs da Cruz *et al.*,[14] and Howell[15] already evidenced the influence of the interatomic potential on the value of the thermal bulk conductivity; therefore, we chose to compare our results only to calculations performed with the same (Tersoff) potential. The direct MD method is used by Abs da Cruz *et al.*[14] with a result of $\kappa_\infty = 125 \pm 6$ W K^{-1}m^{-1} and by Howell[15] with a result of $\kappa_\infty = 155 \pm 4$ W K^{-1}m^{-1}. The difference is attributed by Howell[15] to an underestimation of the error bars in Ref. 14. We did not find any results published using the Tersoff potential with the Green-Kubo method at a temperature of 500 K. Our results are in total agreement with the results by Howell. This agreement validates AEMD as a method to extract thermal conductivities. The theoretical determination keeps higher than the experimental value for natural crystalline Si (Ref. 16) equal to $\kappa_\infty = 80$ W K^{-1}m^{-1}. We believe that the role of the interatomic potential in this discrepancy is crucial. As a matter of fact, interatomic potentials like Tersoff were developed to accurately describe the linear elastic behavior of silicon but the non-linearity of the mechanical response, which should be extremely accurate to give a good estimate of the thermal conductivity, was not explicitly addressed in the design of the potential. A known consequence is the poor quality of the Grüneisen parameters[19] for Tersoff as well as for other potentials like Stillinger-Weber.[20]

We further applied the AEMD method to other materials having significantly different thermal conductivity, namely cGe and α-quartz. The size dependence of the thermal conductivity in these materials at the same temperature (500 K) is summarized in Fig. 5 together with the previous results for cSi. The extrapolation according to Eq. (10) gives $\kappa_\infty = 51 \pm 2$ W K^{-1}m^{-1} and $\lambda = 214 \pm 15$ nm for cGe and $\kappa_\infty = 10.8 \pm 0.3$ W K^{-1}m^{-1}, and $\lambda = 24 \pm 3$ nm for a-quartz along the [001] direction. For these two materials, we could not find in the literature any calculation performed at this temperature. The experiments give a value of $\kappa_\infty = 34$ W K^{-1}m^{-1} for natural, crystalline Ge;[16] experimental data for isotopically pure Ge (Ref. 17) show only a small increase, of about 10%, given the relatively low Debye temperature of cGe (360 K (Ref. 10)). For α-quartz, Pohl *et al.*[18] found a value of 6.5 W K^{-1}m^{-1} at 500 K. In these two cases, the calculation overestimates the value of the thermal conductivity, presumably for the same reason than for cSi, i.e., because of the inability of the interatomic potentials to finely render anharmonicity. Nevertheless, the decrease in thermal conductivity from the cSi to cGe and from cGe to a-quartz is obtained by the calculation, with a ratio equal to 3.0 for $\kappa_\infty^{cSi}/\kappa_\infty^{cGe}$ and 4.8 for $\kappa_\infty^{cGe}/\kappa_\infty^{\alpha-quartz}$ to compare with the experiments equal to 2.3 and 5.2, respectively. The decrease of the length λ from cSi to α-quartz is also qualitatively consistent with the decrease of the maximum phonon mean free paths in less good conductors.

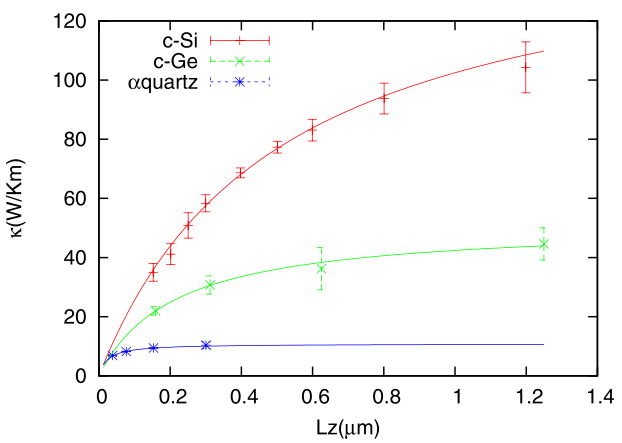

FIG. 5. System size dependence of κ on L_Z for cSi, cGe, and α-quartz. The lines are fits with Eq. (10).

V. CONCLUSIONS

The approach-to-equilibrium MD method (AEMD) is developed, and its connection to the Fourier macroscopic heat equation is explicitly derived. The exponential behavior of the temperature difference, observed between parts of a material initially exposed to a temperature difference, is explained, and the conditions under which a single exponential behavior at long times with a time constant τ is observed are spelled out. In the AEMD method, the temperature is calculated as the average over large ensembles of atoms, and the time constant τ is extracted by an exponential fit of $\Delta T(t)$ over several decades. Once τ is obtained, an explicit expression for the thermal conductivity is derived.

The AEMD approach was applied to cSi. It was shown that the convergence of the conductivity to its asymptotic, size-independent value is improved thanks to the reduced computational cost of the approach. Nevertheless, bulk conductivity in materials with exceedingly long phonon MFPs is out-of-reach even with the present method, but an extrapolation scheme results in an excellent agreement with the results obtained with the direct method and the same interatomic potential. The method is further used to determine the thermal conductivity of less good conductors, cGe and α-quartz. The calculated values systematically overestimate the measured ones, a shortcoming common to other MD methods that must be thought as tools to compare materials or system geometries such as bulk, planes, nanowires, or structuration such as holes rather than quantitative predictors. At least part of the discrepancy between MD calculations and experiments is attributed to the limitations of the interatomic potentials, typically not accurate enough to finely predict the anharmonicity necessary to describe multi-phonon scattering.

Beyond the determination of bulk conductivity, an AEMD approach has been previously applied to the study of interfaces under the lumped capacitance approximation,[21] but it can be easily extended to more general cases. In this perspective, since the AEMD method relies on monitoring just "macroscopic" temperature differences between parts of a system, it is ideally suited for studying atomic-scale systems including complex features, such as nanowires and other discrete nanostructures, disordered or amorphous layers, interfaces with nanoscale roughness, and so on. Therefore, we believe that AEMD can be applied to the study of thermal interface resistances, and could be a fast-computing alternative to study thermal properties in bulk, nanoscale, and interface materials.

ACKNOWLEDGMENTS

Grant to P.A.F. from the French ANR, Project "QUASANOVA" is gratefully acknowledged. This work was granted access to the HPC resources of CINES under the allocation 2013-c2013096939 made by GENCI (Grand Equipement National de Calcul Intensif). We thank S. Volz and D. Donadio for fruitful discussions.

[1]D. G. Cahill, W. K. Ford, K. E. Goodson, G. D. Mahan, A. Majumdar, H. J. Maris, P. Merlin and S. R. Phillpot, J. Appl. Phys. **93**, 793 (2003).
[2]R. Zwanzig, Ann. Rev. Phys. Chem. **16**, 67 (1965).
[3]K. Schelling, S. R. Phillpot, and P. Keblinski, Phys. Rev. B **65**, 144306 (2002).
[4]W. J. Parker, R. J. Jenkins, C. P. Butler, and G. L. Abbott, J. Appl. Phys. **32**, 1679 (1961).
[5]See, for example, T. M. Gibbons and S. K. Estreicher, Phys. Rev. Lett. **102**, 255502 (2009); Z.-Y. Ong and E. Pop, Phys. Rev. B **81**, 155408 (2010); L. Hu, T. Desai, and P. Keblinski, *ibid.* **83**, 195423 (2011).
[6]S. Nosé, Mol. Phys. **52**, 255 (1984); W. G. Hoover, Phys. Rev. A **31**, 1695 (1985).
[7]J. Tersoff, Phys. Rev. B **38**, 9902 (1988).
[8]B. W. H. van Beest, G. J. Kramer, and R. A. van Santern, Phys. Rev. Lett. **64**, 1955 (1990).
[9]I. T. Todorov and W. Smith, The DL_POLY 3 User Manual (Daresbury Lab).
[10]N. W. Ashcroft and N. D. Mermin, *Solid State Physics* (Saunders College Publishing, 1976).
[11]A. J. H. McGaughey and M. Kaviany, Phys. Rev. B **69**, 94303 (2004).
[12]X. W. Zhou, S. Aubry, R. E. Jones, A. Greenstein, and P. K. Schelling, Phys. Rev. B **79**, 115201 (2009).
[13]D. P. Sellan, E. S. Landry, J. E. Turney, A. J. H. McGaughey, and C. H. Amon, Phys. Rev. B **81**, 214305 (2010).
[14]C. Abs da Cruz, K. Termentzidis, P. Chantrenne, and X. Kleber, J. Appl. Phys. **110**, 034309 (2011).
[15]P. C. Howell, J. Chem. Phys. **137**, 224111 (2012).
[16]C. J. Glassbrenner and G. A. Slack, Phys. Rev. **134**, A1058 (1964).
[17]V. I. Ozhogin, A. V. Inyushkin, A. N. Taldenkov, A. V. Tikhomirov, G. E. Popov, E. Haller, and K. Itoh, Pis'ma Zh. Eksp. Teor. Fiz. **63**, 463 (1996). [JETP Lett. **63**, 490 (1996)].
[18]R. O. Pohl, X. Liu, and R. S. Crandall, Curr. Opin. Solid State Mater. Sci. **4**, 281 (1999).
[19]L. J. Porter, J. F. Justo, and S. Yip, J. Appl. Phys. **82**, 5378 (1997).
[20]F. Stillinger and T. Weber, Phys. Rev. B **31**, 5262 (1985).
[21]E. Lampin, Q.-H. Nguyen, P. A. Francioso, and F. Cleri, Appl. Phys. Lett. **100**, 131906 (2012).